

Original Research

Contributions of Diet and Age to Ulcerative Dermatitis in Female C57BL/6J Mice

Alfonso S Gozalo,¹ Patricia M Zerfas,² Jing Qin,³ Derron A Alves,¹ Munir Akkaya,^{4,5}
Mirna Y Peña,⁴ and William R Elkins¹

C57BL/6J (B6) mice are commonly affected by ulcerative dermatitis (UD), a disease of unknown etiology with poor response to treatment. To study the possible role of diet in UD, we compared skin changes in B6 female mice fed a high-fat diet with those of mice fed a control diet. In addition, skin samples from mice with no, mild, moderate, and severe clinical signs of UD were examined by light and transmission electron microscopy (TEM). Mice fed a high-fat diet for 2 mo had more skin mast cell degranulation than did mice fed the control diet for the same period. Regardless of diet, older mice had more skin mast cells and more of these cells were degranulating as compared with younger mice. Microscopic changes in very early lesions were characterized by an increase in dermal mast cells and degranulation with focal areas of epidermal hyperplasia with or without hyperkeratosis. As the condition progressed, a mixed but predominantly neutrophilic inflammatory cell infiltrate appeared in the dermis, with or without epidermal erosion and scab formation. TEM showed that dermal mast cell membranes had disrupted and released a large number of electron-dense granules, whereas degranulated mast cells were filled with isolated and coalescing empty spaces due to fusion of granule membranes. Ulceration appeared to occur very quickly, probably as result of intense scratching due to the pruritogenic properties of the histamine released from mast cell granules. This study showed a direct correlation between dietary fat and skin mast cell degranulation in female B6 mice. In addition, the number of skin mast cells and degranulation rates was higher in older mice. Treatments directed at preventing mast cell degranulation may result in better outcomes when applied early in UD cases. As noted previously in studies using caloric restriction, lower fat content in rodent diets may help prevent UD.

Abbreviations: B6, C57BL/6J; TEM, transmission electron microscopy; UD, ulcerative dermatitis

DOI: 10.30802/AALAS-CM-22-000096

Introduction

C57BL/6 (B6) mice are one of the most common mouse strains used in biomedical research. Unfortunately, this valuable strain and others maintained on this background frequently are affected by ulcerative dermatitis (UD), a condition characterized by skin erosions that typically are located in the interscapular area but can affect any part of the body.^{5,30,40,46} UD usually is accompanied by intense pruritus which leads to self-mutilation resulting in the animal being removed early from study and, in many cases, euthanized due to poor response to treatment.^{5,30,38,40,62} In addition, UD produces reactive immune modulation that can confound research results.^{15,29} The etiology of UD remains unknown but is suspected to be multifactorial with a genetic predisposition and secondary to a variety of conditions including mite infestation, staphylococcal infection, immune complex vasculitis, vitamin A toxicity, and behavioral and environmental factors.^{5,14,16,38,40,49,54-57,62} Calorie-restricted diets have long been noted to reduce UD incidence while high-fat

diets appear to exacerbate the condition.^{9,29,50,51,53,61} The highest UD incidence is reported in mice older than 1 y, with inconsistent predilection for female mice.^{9,61} Several different treatment options have been proposed, but none have proven to be 100% effective.^{1,2,18,29,40,44,46,63}

To study the possible role of diet in UD, we compared skin changes in B6 mice fed a high-fat diet with those of mice fed a control diet. In addition, skin samples from B6 mice with no, mild, moderate, and advanced clinical signs of UD were examined by light and transmission electron microscopy (TEM) in an effort to better characterize the various stages of the disease, its pathogenesis, and its possible etiology.

Materials and Methods

Animals. Mice were housed at the National Institute of Allergy and Infectious Diseases, National Institutes of Health, an AAALAC-accredited barrier facility, as part of several IACUC-approved experimental protocols. The mice were cared for according to the *Guide for the Care and Use of Laboratory Animals*³³ and Animal Welfare Regulations.^{6,7} Husbandry included the use of ventilated microisolators (Lab Products, Seaford, DE) as sterile cage setups with autoclaved hardwood bedding (SaniChip, Harlan Teklad, Madison, WI) and with autoclaved food (our standard feed; LabDiet Verified 75 IF/Auto Ext Mod 5V0T, LabDiet, St Louis, MO) and acidified drinking water provided ad libitum. Room temperature was maintained between

Submitted: 23 Aug 2022. Revision requested: 14 Sep 2022. Accepted: 23 Nov 2022.

¹Comparative Medicine Branch, National Institute of Allergy and Infectious Diseases; ²Pathology Service, Office of Research Services; ³Biostatistics Research Branch, National Institute of Allergy and Infectious Diseases, and ⁴Laboratory of Immunogenetics, National Institute of Allergy and Infectious Diseases, National Institutes of Health, Bethesda, Maryland; and ⁵Department of Internal Medicine, Division of Rheumatology and Immunology, Department of Microbial Infection and Immunity, Pelotonia Institute for Immuno-Oncology, Columbus, Ohio.

20.0 and 23.3 °C, relative humidity between 30% and 50%, and light on a 14:10-hr light:dark cycle (lights on from 0600 to 2000). Sentinel mice were tested quarterly for excluded rodent pathogens including mouse hepatitis virus, pneumonia virus of mice, Sendai virus, Theiler murine encephalomyelitis virus, mouse rotavirus, lymphocytic choriomeningitis virus, ectromelia virus, mouse cytomegalovirus, minute virus of mice, polyoma virus, reovirus 3, mouse adenovirus, rodent parvoviruses, *Mycoplasma pulmonis*, and cilia-associated respiratory bacillus. Hantavirus testing was done once a year, and endoparasite and ectoparasite examinations were performed every 6 wk. Mouse norovirus and *Helicobacter* spp. were not excluded from the colony, and so all mice were considered potentially infected with these agents. Euthanasia was performed by using CO₂ overdose consistent with the American Veterinary Medical Association guidelines on euthanasia.³

Diet study. Research-naïve and dermatitis-free female C57BL/6J mice (age, 2 mo) were fed a commercial, high-fat rodent diet (D12492, Research Diets, New Brunswick, NJ) or a control diet (D12450J, Research Diets) for 2 mo (8 mice per group) or 10 mo (9 mice on high-fat diet and 5 mice on control diet) as part of an IACUC-approved study. The mice were then euthanized, and dorsal interscapular skin samples were collected, fixed in 10% neutral-buffered formalin, embedded in paraffin, sectioned at 5 µm, and stained for light microscopy examination with hematoxylin and eosin, Giemsa, and toluidine blue using routine methods. The skin sections were evaluated for morphologic changes and inflammation. Total and degranulating mast cells were counted in 5 randomly selected high-power fields (magnification, ×400) per section.

Light microscopy and TEM. Research-naïve adult female C57BL/6J mice ($n = 28$) were euthanized, and skin samples were collected; 14 mice had clinical signs of dermatitis, found during daily rounds by health technicians, and 14 had no gross skin lesions. The ages of the mice ranged between 81 and 247 d. The mice had been fed either a standard diet (5V0T, Verified 75 IF/Auto Ext Mod, LabDiet, St Louis, MO; $n = 5$), a high-fat diet (D12492, Research Diets; $n = 9$), or a control diet (D12450J, Research Diets; $n = 14$). The skin lesions were categorized by the attending veterinarian based on the character and size of the lesion as mild (single excoriation or crust, 5 mm or less in diameter), moderate (multiple or coalescing crusts expanding more than 5 mm but less than 2 cm in diameter), or severe (single or multifocal erosions or ulcerations affecting an area 2 cm or more in diameter or effacing several skin layers). Of the 14 mice with clinical dermatitis, 4 were categorized as mild, 6 as moderate, and 4 as severe. Mice fed the standard diet had one mild, one moderate, and one severe UD case; mice on high-fat diet had 4 moderate and 2 severe UD cases; and mice fed the control diet had 3 mild, one moderate, and one severe UD case. All mice with moderate UD were at least 4 mo old, and those with severe UD were at least 6 mo of age. Only skin lesions affecting the nape of neck, interscapular region, or dorsum were collected; skin lesions affecting other areas of the body were not used in this study to avoid including lesions caused by excessive grooming or fighting or ear tag allergy.³⁷

Samples were fixed in 10% neutral-buffered formalin and processed for light microscopy as described earlier. Skin samples from 4 selected cases were fixed in 2% glutaraldehyde and 1% paraformaldehyde and processed for TEM examination. The fixed skin samples were washed with 0.1 M cacodylate buffer (pH 7.4), fixed with 1% OsO₄, washed again with cacodylate buffer, washed with water, and placed in 1% uranyl acetate for 1 h. The tissues were subsequently serially dehydrated

in ethanol and propylene oxide and embedded in resin (EM-Bed 812, Electron Microscopy Sciences, Hatfield, PA). Thin sections, approximately 80 nm, were obtained by using an ultramicrotome (Ultracut-UCT, Leica, Deerfield, IL), placed onto 300-mesh copper grids, stained with saturated uranyl acetate in 50% methanol, and then stained with lead citrate. The grids were viewed on an electron microscope (JEM-1200EXII, JEOL, Tokyo, Japan) at 80 kV, and images were recorded by using a midmounted 10.5 MP CCD camera (XR611M, Advanced Microscopy Techniques, Danvers, MA).

Statistical analysis. Comparisons between diet groups were conducted by using 2 sample t tests. The binomial likelihood ratio statistic was used to analyze the ratio of degranulating cells. Due to the variable cluster size of cells, the permutation method was used to evaluate the significance between the ages of 2 and 10 months. All calculations were done by using the statistical software package R (version 4.1.3; R Core Team, Vienna, Austria).

Results

Diet study. None of the mice in the high-fat or control diet groups developed gross skin lesions. Microscopically, the epidermis was 1 or 2 cell layers consisting of stratum basale (basal cell layer) with occasional desquamation of epithelial cells. The dermis, composed of fibroblasts (and variable number of mast cells) separated by dermal collagen, supports adnexal structures (that is, hair follicles, sebaceous glands), blood vessels, arrector pili muscle, and peripheral nerves overlying the panniculus adiposus and panniculus carnosus (striated muscle). Mice fed the high-fat diet for 2 or 10 mo had similar numbers of dermal mast cells as the controls (2 mo: average, 43 cells compared with 36 cells [$P = 0.13$]; 10 mo: average, 95 cells compared with 59 cells [$P = 0.12$]; Figure 1; Tables 1 through 4). The mean ratio of degranulating mast cells per total mast cells was significantly higher in mice fed a high-fat diet for 2 mo (0.587) compared with mice fed the control diet for 2 mo (0.24; $P = 0.0015$; Figure 2). However, the mast cell degranulation ratio of mice fed the high-fat feed for 10 mo (0.733) was similar to that of mice fed the control diet for 10 mo (0.633; $P = 0.1033$; Figure 2). When we compared mice fed the control diet, older mice had

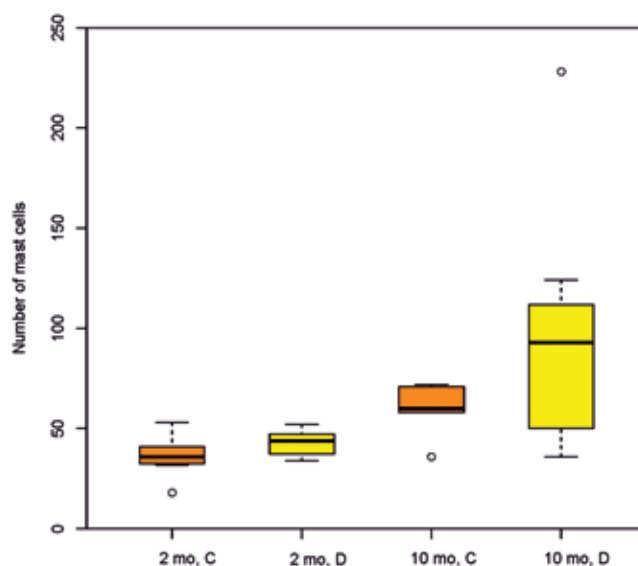


Figure 1. Number of skin mast cells in mice fed the control diet (C) or high-fat diet (D) for 2 or 10 mo. Empty dots represent outliers.

Table 1. Skin mast cells in mice fed control diet for 2 mo

Mouse	Mast cells		
	Total no.	No. degranulating	% degranulating
1	33	4	12
2	18	4	22
3	34	10	29
4	41	8	19
5	53	7	13
6	38	18	47
7	32	3	9
8	41	16	39
Overall	290 (\bar{x} = 36.25)	70 (\bar{x} = 8.75)	24

Cells in 5 randomly selected high-power fields (magnification, 400 \times) were counted per section.

Table 2. Skin mast cells in mice fed high-fat diet for 2 mo

Mouse	Mast cells		
	Total no.	No. degranulating	% degranulating
1	52	18	35
2	44	17	39
3	34	23	68
4	48	29	60
5	44	25	57
6	37	28	76
7	38	25	66
8	47	33	70
Overall	344 (\bar{x} = 43.00)	198 (\bar{x} = 24.75)	58

Cells in 5 randomly selected high-power fields (magnification, 400 \times) were counted per section.

Table 3. Skin mast cells in mice fed control diet for 10 mo

Mouse	Mast cells		
	Total no.	No. degranulating	% degranulating
1	60	31	52
2	72	46	64
3	36	23	64
4	58	46	79
5	71	41	58
Overall	297 (\bar{x} = 59.40)	187 (\bar{x} = 37.40)	63

Cells in 5 randomly selected high-power fields (magnification, 400 \times) were counted per section.

significantly more skin mast cells (average, 59 cells) than younger mice (average, 36 cells; $P = 0.0186$; Figure 1). Likewise, among mice fed the high-fat diet, older mice had significantly more skin mast cells (average, 95 cells) than younger mice (average, 43; $P = 0.03$; Figure 1). The mean ratio of degranulating cells per total mast cells in mice fed the control diet for 10 mo was significantly higher than for mice fed the control diet for 2 mo (0.633 compared with 0.240; $P < 0.001$; Figure 2). The mean ratio of degranulating cells per total mast cells in mice fed the high-fat diet for 10 mo was significantly higher than in mice fed the high-fat diet for 2 mo (0.734 compared with 0.587; $P = 0.03$; Figure 2).

The mean ratio of degranulating mast cells per total mast cells in mice fed the control diet for 2 mo was divided by the mean ratio in mice fed the high-fat diet for 2 mo, resulting in a ratio of

Table 4. Skin mast cells in mice fed high-fat diet for 10 mo

Mouse	Mast cells		
	Total no.	No. degranulating	% degranulating
1	63	51	81
2	124	97	78
3	50	38	76
4	112	83	74
5	48	37	77
6	36	25	69
7	93	59	63
8	228	185	81
9	97	58	60
Overall	851 (\bar{x} = 94.56)	633 (\bar{x} = 70.33)	74

Cells in 5 randomly selected high-power fields (magnification, 400 \times) were counted per section.

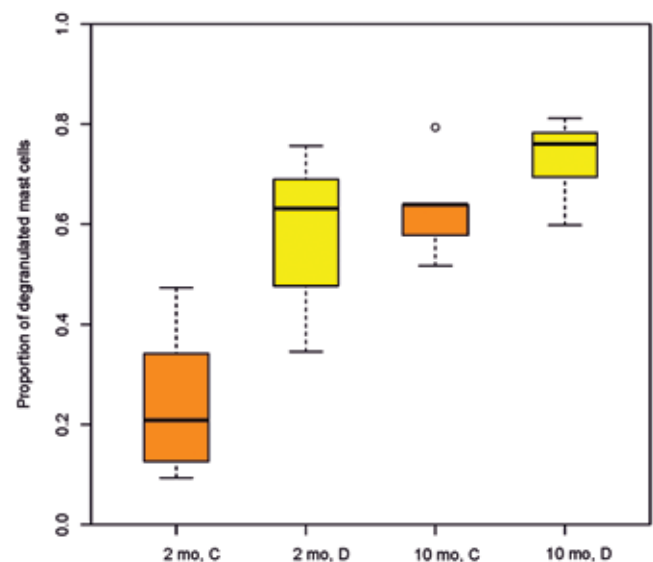


Figure 2. Mean ratio of degranulating mast cells per total mast cells in mice fed the control diet (C) or high-fat diet (D) for 2 or 10 mo. Empty dots represent outliers.

ratios value of 0.410. At 10 mo, the mean ratio of degranulating per total mast cells in mice fed the control diet was divided by the mean ratio in mice fed high-fat diet, resulting in a ratio of ratios value of 0.863. When we compared both ratio of ratios (0.410 compared with 0.863), we found a significant difference ($P < 0.001$) between the 2, such that older mice had a larger ratio of ratios of degranulating mast cells, and younger mice had a larger change of ratios (ratio between control and high fat diet) compared with the older group (Figure 2). Older mice had more skin mast cells and more were degranulating as compared with younger mice (Figure 3 A through F).

All skin samples from mice fed the high-fat diet for 2 mo floated when placed in fixative, whereas skin samples from mice fed the control diet sank to the bottom of the jar. Skin samples from older mice, regardless of diet, floated when placed in fixative. On histologic examination, older mice had a thicker layer of subcutaneous adipose tissue, with larger diameter adipocytes, than did younger mice (Figure 3 A and C). Sebaceous glands in older mice, particularly among those fed the high fat diet, were also larger than in younger mice. Three mice fed the high-fat diet for 10 mo showed multifocal epidermal hyperplasia with

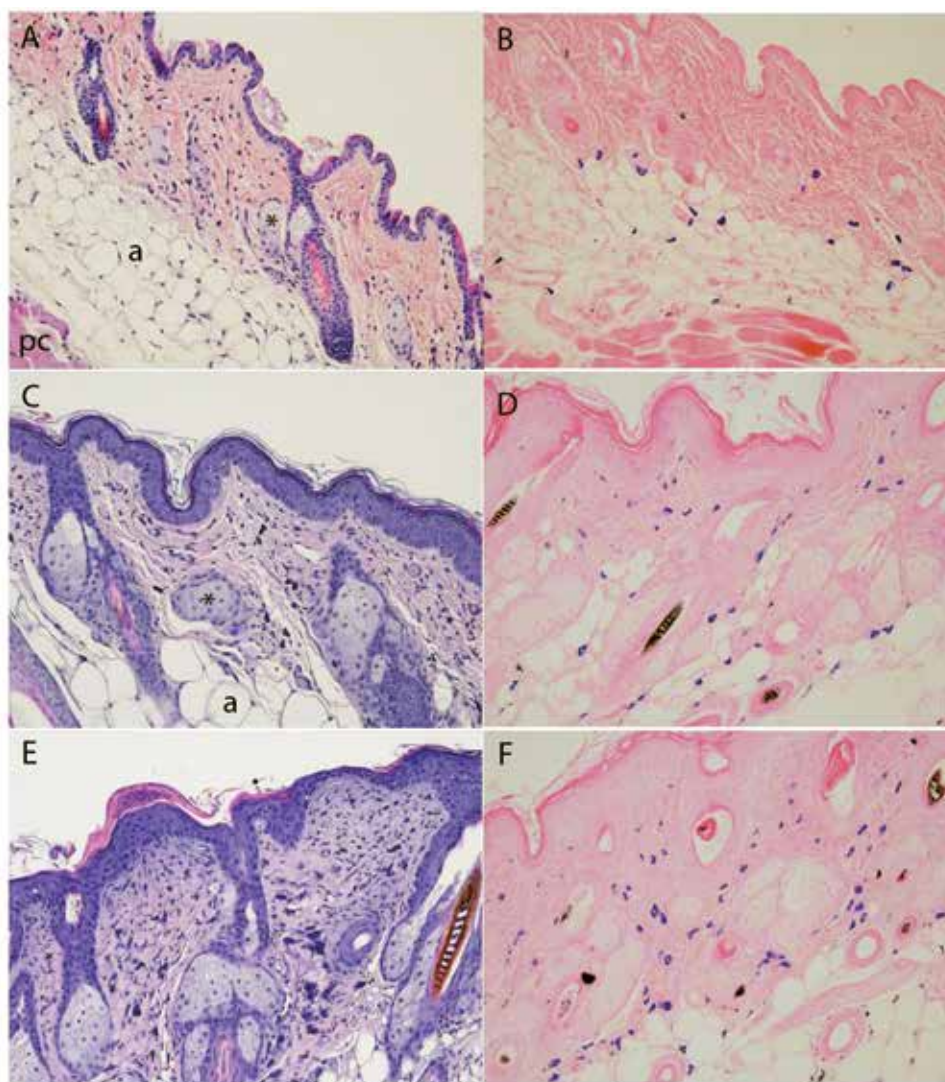


Figure 3. (A) Mouse, skin. Mouse fed control diet for 2 mo showing a 1- to 2-cell-layer epidermis, with a thin surface keratin layer and the dermis containing fibroblasts, collagen fibers, mast cells, hair follicles, sebaceous glands (*), small blood vessels, peripheral nerves, adipocytes (a), arrector pili muscle, and a skeletal muscle, the panniculus carnosus (pc). Hematoxylin and eosin stain; magnification, 100 \times . (B) Mouse, skin. Mouse fed control diet for 2 mo. showing a few dermal mast cells (cells stained dark blue) with very few degranulating. Toluidine blue stain; magnification, 100 \times . (C) Mouse, skin. Mouse fed high-fat diet for 10 mo, showing epidermal hyperplasia, increased number of dermal mast cells and larger adipocytes (a) and sebaceous glands (*) compared with younger mice on control diet (panel A). Hematoxylin and eosin stain; magnification, 100 \times . (D) Mouse, skin. Mouse fed high-fat diet for 10 mo, showing an increase in dermal mast cells (cells stained dark blue), many of them degranulating, compared with young mice on control diet (panel B). Toluidine blue stain; magnification, 100 \times . (E) Mouse, skin. Mouse fed high-fat diet for 10 mo, showing epidermal hyperplasia with hyperkeratosis, dermal thickening and fibrosis, and increased mast cell degranulation compared with younger mice on control diet (panel A). Hematoxylin and eosin stain; magnification, 100 \times . (F) Mouse, skin. Mouse fed high-fat diet for 10 mo, showing significantly more dermal mast cells (cells stained dark blue), many of them degranulating, compared with young mice on control diet (panel B). Toluidine blue stain; magnification, 100 \times .

or without mild hyperkeratosis; this change was not observed in any of the mice in the other groups (Figure 3 C and E).

Light microscopy. Histologic examination showed that, among the 14 mice with no gross skin abnormalities, 5 (36%) had noteworthy changes. These very early skin lesions were in superficial and deep layers of the dermis and were characterized by focal areas of epidermal hyperplasia, sometimes with parakeratotic to orthokeratotic hyperkeratosis, and by more mast cells, many of them degranulating, as was seen in some of the mice on the high-fat diet study (Figure 3 E and F). As the condition progressed, spongiosis of the epidermal basal cell layer was evident and was accompanied by a mixed dermal inflammatory cell infiltrate composed mainly of neutrophils and lymphocytes but also with plasma cells and occasional eosinophils with or without epidermal surface erosion and scab

formation (Figure 4 A and B). In affected areas, the majority of the mast cells were degranulating. Dermal fibrosis and a mixed inflammatory infiltrate increased with UD severity (Figure 4 B and C). Keratinocyte mitotic figures were more common in hyperplastic epidermal areas next to moderate to severe UD. In a few cases, hair follicles were cystic in areas of severe inflammation, but hair follicles in adjacent dermis were normal. No vascular or sebaceous gland lesions were noted. Advanced cases showed large areas of epidermal serocellular crusts, with hyperkeratosis, large areas of ulceration or both, with extension into the deep dermis. Within the affected dermis, numerous reactive fibroblasts (that is, fibroplasia) and small-caliber vessels were effacing and replacing adnexal structures and extending through the panniculus carnosus in some areas. The small-caliber vessels were often oriented perpendicular to the ulcerated

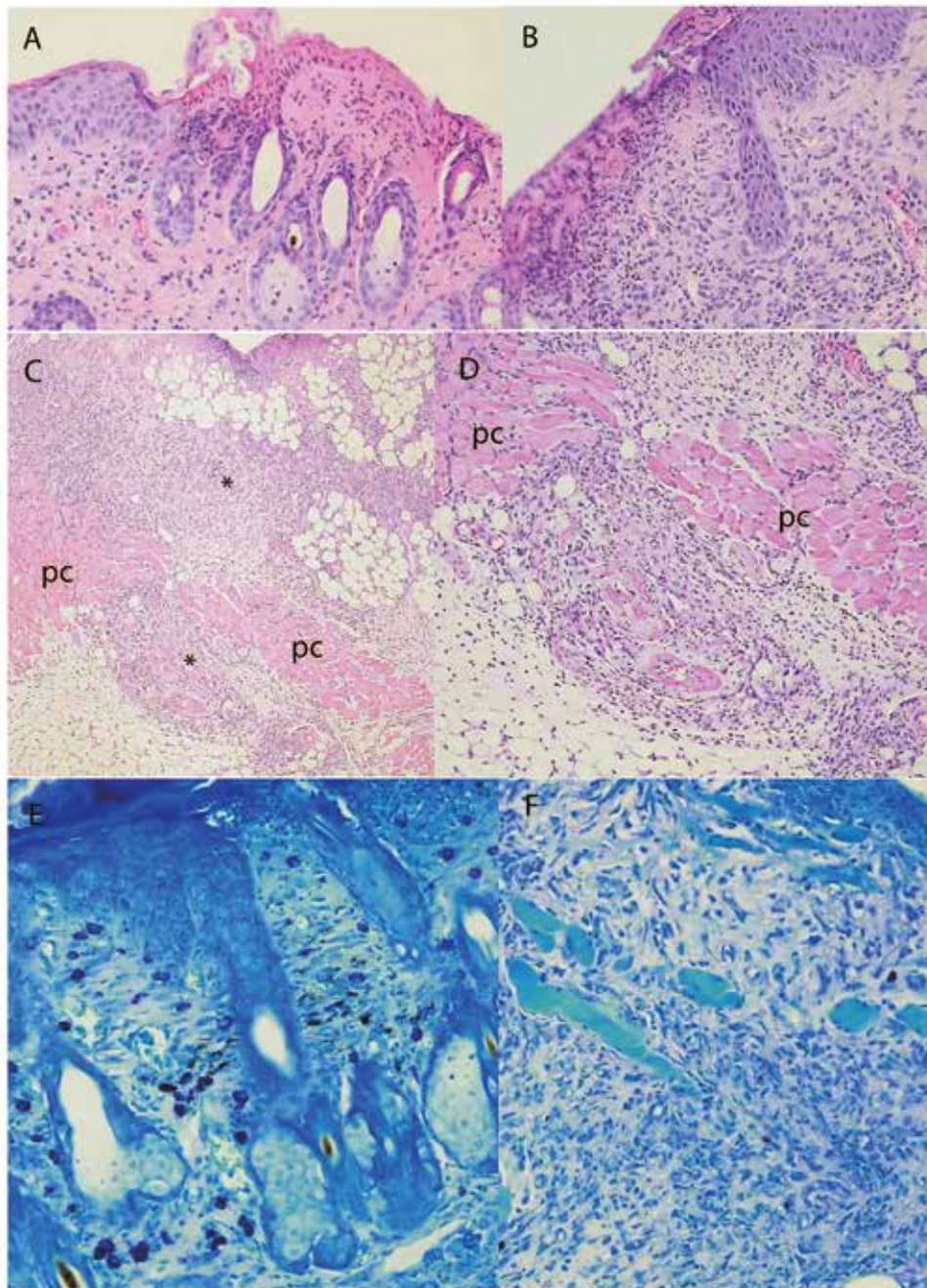


Figure 4. (A) Mouse, skin. Mild UD characterized by epidermal hyperplasia and ulceration with thin serocellular crust formation and mild dermal inflammatory infiltrate. Hematoxylin and eosin stain; magnification, 200 \times . (B) Mouse, skin. Moderate case of UD with epidermal hyperplasia, ulceration, and an extensive inflammatory infiltrate, composed mainly of neutrophils and mast cells. Hematoxylin and eosin stain; magnification, 200 \times . (C) Mouse, skin. Low-power image showing severe UD with a large area of epidermal full thickness ulceration with marked inflammatory infiltrate, extensive fibroplasia, and granulation tissue that effaces and replaces adnexal structures and extends into the deep dermis and through the panniculus carnosus (pc). Hematoxylin and eosin stain; magnification, 40 \times . (D) Mouse, skin. Same section as panel C but at higher magnification showing the inflammation and granulation tissue extending past the panniculus carnosus (pc). Hematoxylin and eosin stain; magnification, 100 \times . (E) Mouse, skin. Section showing epidermal ulceration with large numbers of degranulating dermal mast cells (mast cell granules are stained deep purple). Histologically normal adnexal structures are still present. Giemsa stain; magnification, 200 \times . (F) Mouse, skin. Same section as panel C showing extensive granulation tissue with no visible mast cells across the section as evidenced by absence of mast cell granule staining. Giemsa stain; magnification, 200 \times magnification.

surface (consistent with granulation tissue) and were admixed with the previously described mixed inflammatory infiltrate (Figure 4 C through F). Acanthosis and hyperkeratosis were common adjacent to ulcerated areas. No microscopic evidence of bacterial, mycotic, viral, or parasitic infection was noted in these tissues under light microscopy.

TEM. As with light microscopy, TEM revealed that the epidermis in nonaffected areas was 1 or 2 cells in thickness, with a basal cell layer and a thin surface horny cell layer. Stacking of keratinocytes for up to 4 or 5 layers (mild epidermal hyperplasia), often with 2 or 3 prominent nucleoli in cells, was a very early finding (Figure 5 A through C). In addition, mild intercellular edema (spongiosis) evidenced by increased

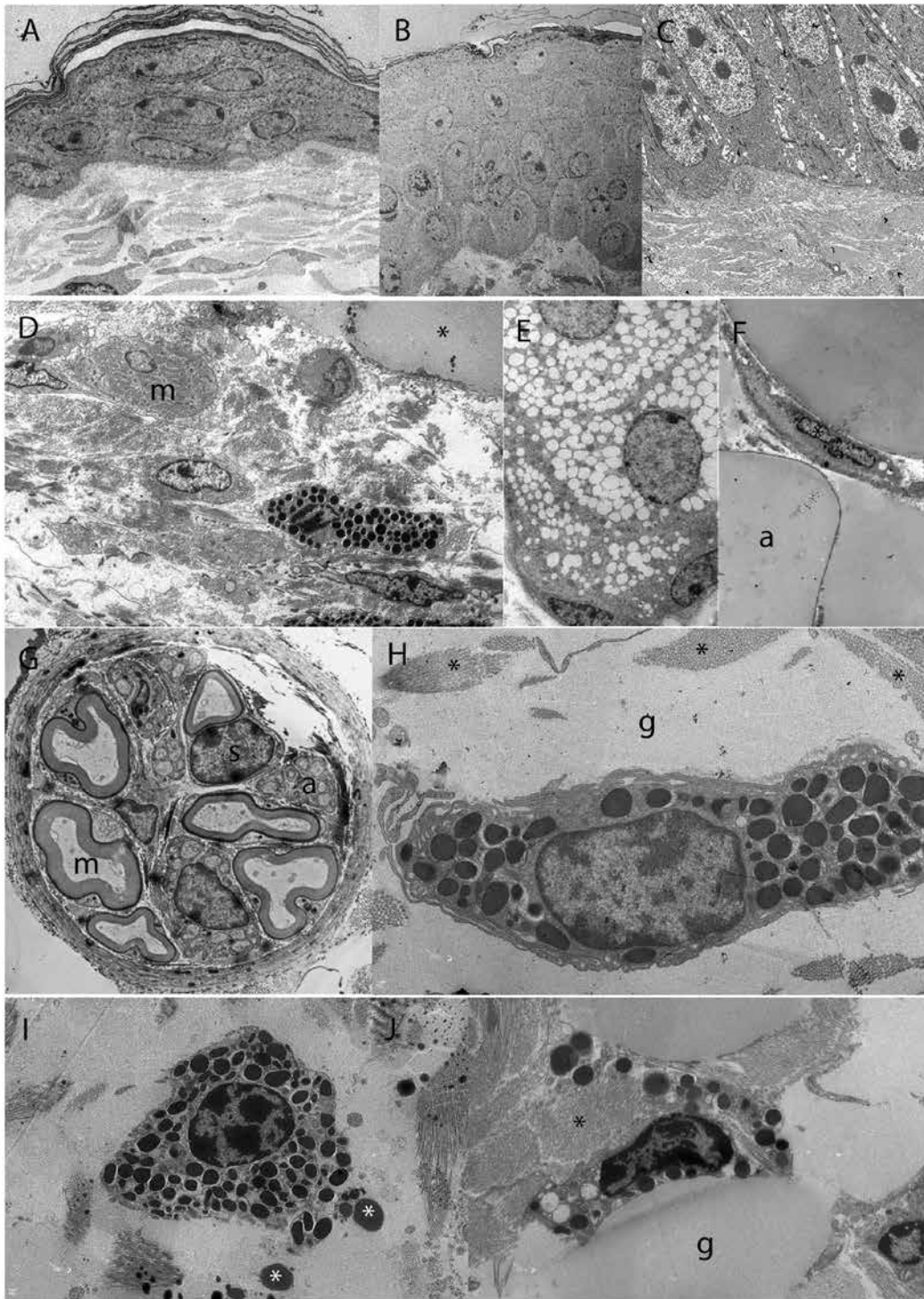


Figure 5. (A) Mouse, skin. Mouse with no dermatitis showing 2- to 3-cell-layer epidermis with a thin surface keratin layer and the dermis composed of ground substance, collagen bundles, and a fibroblast. Uranyl acetate and lead citrate stain; magnification, 1200 \times . (B) Mouse, skin. Early subclinical dermatitis characterized by epidermal hyperplasia. Uranyl acetate and lead citrate stain; magnification, 1400 \times . (C) Mouse, skin. Early subclinical dermatitis characterized by epidermal hyperplasia with basal keratinocytes containing multiple nucleoli and mild separation of the intercellular gaps by edema. Uranyl acetate and lead citrate stain; magnification, 1200 \times . (D) Mouse, dermis. Normal dermis showing resting mast cells containing numerous electron-dense granules, fibroblasts, collagen fibers, skeletal muscle (m), and lipid globule (asterisk). Uranyl acetate and lead citrate stain; magnification, 1000 \times magnification. (E) Mouse, dermis. Multiple sebocytes, as part of a normal sebaceous gland, containing cytoplasmic lipid droplets. Uranyl acetate and lead citrate stain; magnification, 2000 \times . (F) Mouse, dermis. Normal small blood vessel (asterisk) between adipocytes (a). Note the adipocyte thin cell membrane. Uranyl acetate and lead citrate stain; magnification, 1000 \times . (G) Mouse, dermis. Cross section of a normal peripheral nerve showing Schwann cells (s), unmyelinated axons (a), and myelinated axons (m). Uranyl acetate and lead citrate stain; magnification, 4800 \times . (H) Mouse, dermis. Normal resting mast cell surrounded by ground substance (g) and collagen bundles (*). Uranyl acetate and lead citrate stain; magnification, 3000 \times . (I) Mouse, dermis, mild UD. Activated mast cell showing a few extruded granules becoming less electron dense as they swell and dissolve (white *). Uranyl acetate and lead citrate stain; magnification, 2000 \times . (J) Mouse, dermis, moderate UD. Actively degranulating mast cell surrounded by collagen bundles (*) and ground substance (g). Note an adipocyte nucleus on lower right corner. Uranyl acetate and lead citrate stain; magnification, 2500 \times .

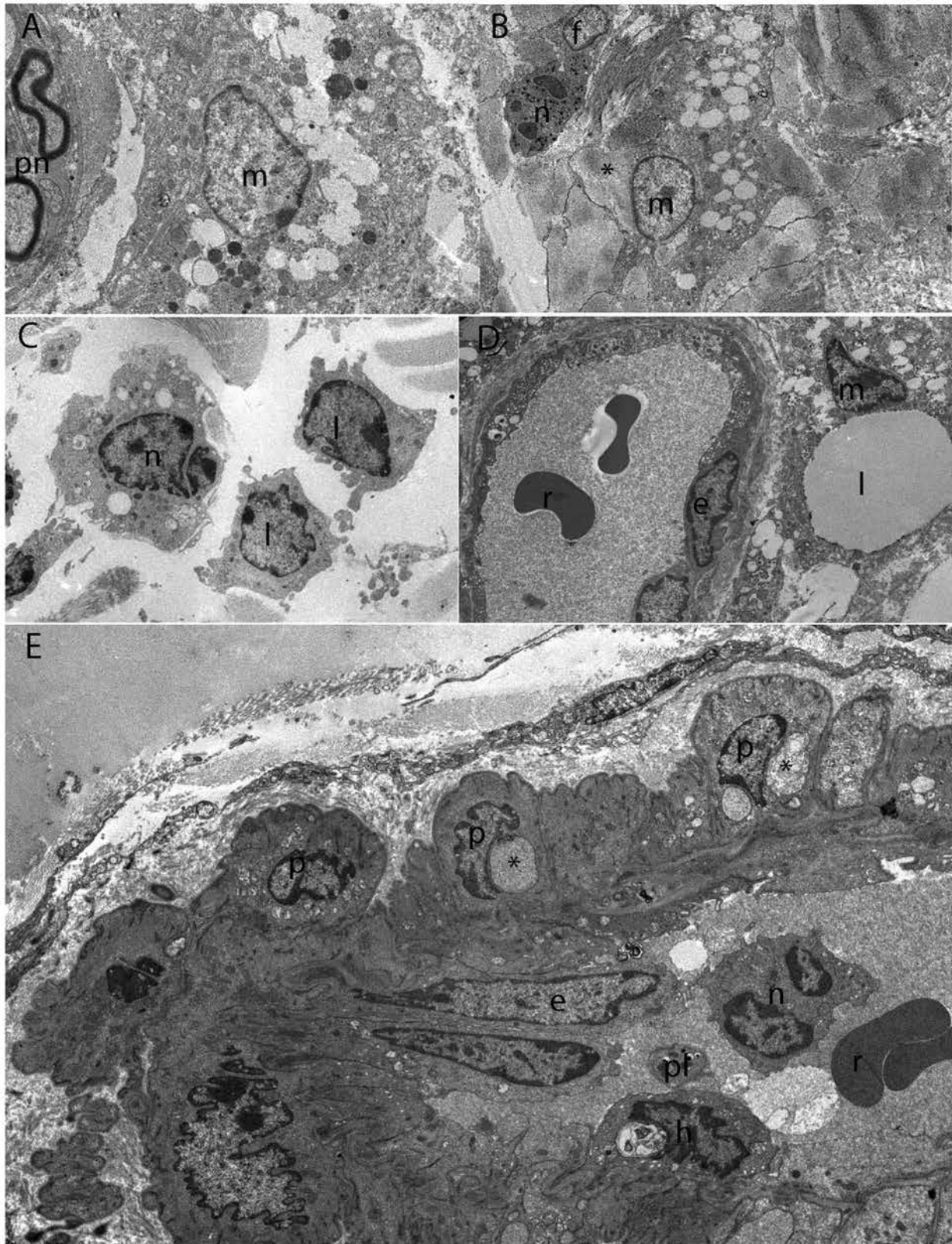


Figure 6. (A) Mouse, dermis, moderate UD. A completely degranulated mast cell (m) next to a myelinated peripheral nerve (pn). Uranyl acetate and lead citrate stain; magnification, 2000 \times . (B) Mouse, dermis, moderate UD. Completely degranulated mast cell (m) surrounded by large amounts of collagen (asterisk) and next to a neutrophil (n) and fibroblast (f). Note the fine fibroblast cytoplasmic extensions. Uranyl acetate and lead citrate stain; magnification, 1500 \times . (C) Mouse, dermis, moderate UD. Active neutrophil (n) and lymphocytes (l). Uranyl acetate and lead citrate stain; magnification, 1500 \times . (D) Mouse, dermis, moderate UD. Degranulated mast cell (m) next to a small blood vessel containing red blood cells (r) and metabolically active vascular endothelial cells (e). Note a lipid globule next to the blood vessel (l). Uranyl acetate and lead citrate stain; magnification, 1200 \times . (E) Mouse, dermis, severe UD. Small blood vessel showing pericyte (p) contraction with marked organelle swelling (*). Endothelial cells (e) appear to be protruding into the vascular lumen, possibly an effect of the section. Note intraluminal red blood cells (r), a neutrophil (n), a platelet (pl), and a phagocytic histiocyte (h) apparently attached to the vascular endothelium. Uranyl acetate and lead citrate stain; magnification, 1200 \times .

separation between keratinocytes, was also a consistent finding, particularly in the stratum basale (Figure 5 C). In the dermis of very early cases, no significant ultrastructural findings were associated with resident dermal cells (that is, fibroblasts, adipocytes), cells of the pilosebaceous unit (for example, hair follicles, sebaceous glands), supporting structures (for example, blood vessels, peripheral nerves, skeletal muscle), and the surrounding collagen and ground substance (Figure 5 D through H). However, the numbers of mast cells were slightly elevated, with many of them degranulating (Figures 5 I and J and 6 A). Consistent with light microscopy findings, in more advanced stages, infiltrating inflammatory cells, mainly neutrophils, lymphocytes, and occasional plasma cells and histiocytes were seen in the dermis (Figure 6 B and C), with significant amounts of cell debris and fragmented collagen fibrils (suggestive of collagen lysis), especially in ulcerated areas. Elevated numbers of degranulating mast cells were also seen and were commonly found close to small blood vessels and nerves (Figure 6 A and D). Mast cell membranes were disrupted by fusion of the granule and plasma membranes, with lysis resulting in the release of numerous electron-dense intact granules into the extracellular space. Extruded granules were swollen and became less electron-dense as they appeared to dissolve. After complete degranulation, the mast cells contained isolated and coalescing empty spaces as result of granule membrane fusion (Figure 6 A and B). Vascular lesions characterized by pericyte contraction with marked organelle swelling (Figure 6 E) were occasionally seen in the most affected areas. No parasitic, bacterial, mycotic, or viral agents were noted in the examined skin samples, nor were cryoglobulins crystals or other cell inclusions observed.

Discussion

The earliest reference to dermatitis in C57BL/6 mice appears to be in 1954 when an investigator reported on pyridoxine deficiency studies: “with chronic deficiency, C57BL developed a dermatitis not seen in other strains.”¹⁷ Since then, many reports have described UD in B6 mice associated with a variety of conditions, but high-fat diets have consistently been associated with a greater incidence of UD, whereas calorie-restricted diets are reported to reduce the incidence.^{9,29,50,51,53,61} The condition is common in B6 mice, responds poorly to treatment, and has an undefined etiology and poorly understood pathogenesis. To study the possible role of diet in UD, we compared skin changes in B6 mice fed a high-fat diet with those of mice fed a control diet. In addition, we examined skin samples from B6 mice with no, mild, moderate, and severe clinical signs of UD by light microscopy and TEM in an effort to better characterize the various stages of the disease, its pathogenesis, and its possible etiology.

Our findings from both light microscopy and TEM suggest that the initial changes leading to UD in C57BL/6J female mice were characterized by an increase in intact and degranulating dermal mast cells followed by epidermal hyperplasia. Ulceration appears to occur very quickly, probably as result of intense scratching due to the pruritogenic properties of the histamine released from mast cell granules.¹² Histamine may also be responsible for the epidermal hyperplasia noted in some mice without skin ulceration, because histamine has been shown to stimulate keratinocyte proliferation.^{8,22} Histamine dilates postcapillary venules, activates the endothelium, and promotes blood vessel permeability, leading to local edema, warmth, redness, and the influx of other inflammatory cells to the site of release.^{12,31} Histamine also depolarizes nerve endings, leading to itching or pain.^{13,59} In addition to histamine, mast cell granules can also contain or produce serotonin, heparin, prostaglandins,

and leukotrienes as well as mast cell-specific enzymes, including chymases, tryptases, and carboxypeptidase A, and several pro- and anti-inflammatory cytokines, including TNF α and IL6.^{23,31} Furthermore, mast cells produce and release type 2 cytokines, including IL4, IL13, thymic stromal lymphopoietin, periostin, IL25, IL31, and IL33.^{15,21,32,48} Histamine released from mast cells reacts with skin nerve fibers, leading to induction of itch, and activates them to release neuropeptides (e.g., substance P), which in turn elicit the release of histamine and other pro-inflammatory substances from mast cells and leukotriene B4 from keratinocytes and perpetuate the itch-scratch cycle.^{4,59} Scratching also promotes keratinocyte release of proinflammatory cytokines, chemokines, and antimicrobial peptides that promote T cell and innate immune cell infiltration.^{20,21,41,48,64} More specifically, in response to scratch injury, keratinocytes produce and release CXC-motif chemokine ligand 8 (CXCL8) and CC-motif chemokine ligand 20 (CCL20), which are potent chemoattractants for neutrophils and IL17A-producing immune cells, respectively.²⁰ This mechanism is consistent with previous studies of UD in B6 mice that have shown neutrophils and mast cells as the predominant inflammatory cells in skin lesions, together with elevations in IL6, TNF α , IL1 β , and keratinocyte-derived cytokine.^{5,15,29,30,38,40,62} IL6 induces the infiltration of mononuclear cells and is believed to be important in ongoing chronic skin irritation, whereas TNF α upregulates proinflammatory cytokines and adhesion molecules on keratinocytes and vascular endothelial cells, facilitating the migration and adhesion of inflammatory cells in the epidermis.³⁴ Keratinocyte-derived cytokine, also known as CXCL1, contributes to neutrophil chemotaxis and activation,²⁰ whereas IL25, produced by mast cells and nonimmune cells in the skin, stimulates dermal dendritic cells to produce IL1 β , contributing to activation and enhancement of a Th17 cell-mediated response.⁵⁸ As noted previously by others, the changes in cytokine content in B6 mice with UD are consistent with the Th2 and Th17 differentiation seen in humans with atopic dermatitis.^{15,29}

The apparent reduction in the number of mast cells in severe UD cases may indicate that most of the mast cells in the affected area had already degranulated and were difficult to distinguish from other mononuclear inflammatory cells by light microscopy. Mast cell identification by light microscopy is based on the characteristic staining properties of their cytoplasmic granules, which is lost once the mast cell is completely degranulated. Some mice had areas of alopecia, but these were not correlated with dermatitis or hair shaft abnormalities on microscopic examination. Cases of severe UD may heal with extensive scarring due to fibroplasia and fibrosis replacing normal dermal structures which, depending on location, may interfere with the animal's ambulation due to tissue contraction. Further supporting the role of mast cells in UD, reports of treatments with some success all to some degree attenuate mast cell degranulation or modulate pathways that cause mast cell activation or inhibit the itch-scratch cycle. For example, vitamin E and mineral dietary supplementation with calcium both attenuate mast cell activation.^{24,65} Maropitant citrate dampens the itch-scratch cycle and appears to have anti-inflammatory effects.⁶⁰ Ibuprofen reduces inflammation and pain but also relieves pruritus in patients with mast cell activation syndrome,³⁶ and highly diluted sodium hypochlorite is used as an antiseptic in wound care but also induces various cellular pathways that contribute to attenuation of the inflammatory response and lessening of itching.³⁹ Nail trimming may blunt damage from scratching that results in keratinocyte release of proinflammatory mediators and thus limit further trauma to the skin; this action may promote

healing in mice with UD.^{20,21,48} However, most treatments are applied when UD is noted clinically, which occurs after other inflammatory cells, apart from mast cells, already are engaged and actively contributing to UD. Some reports suggest that female B6 mice are more prone to UD than are males; a possible explanation for this difference is that testosterone leads to the expression of mast cell IL33, activation of type 2 innate lymphoid cells, and priming of Th2 cell responses.¹² Females do not express the threshold level of testosterone needed to activate the Th2 pathway, resulting in a predominantly more pathogenic Th17 cell response. As testosterone levels fall with age in males, so does mast cell IL33 expression and reversion to a predominantly Th17 response,¹² thus perhaps explaining in part why UD incidence increases with age in B6 males.

Several studies have shown that high-fat diets may exacerbate UD in B6 mice, whereas low-calorie and restricted diets may lower the incidence.^{9,29,50,51,53,61} Our study suggests that high-fat diets may exacerbate UD by causing an increase in the total number and number of degranulating mast cells in the dermis, which promotes epidermal hyperplasia and scratching; this effect in turn activates keratinocytes to produce and release proinflammatory cytokines, chemokines, and antimicrobial peptides attracting inflammatory cells. The intense scratching results in trauma to the skin with consequent ulceration, which further attracts inflammatory cells and may allow secondary bacterial infections, most commonly *Staphylococcus xylosum*.³⁸

The mechanism by which high-fat diets cause an increase in dermal mast cells and degranulation ratio may be associated with the type and amount of essential fatty acids in commercial rodent diets. The suggested optimal n-6:n-3 fatty acid ratio for rodent diets is between 1 and 6.^{10,11,42} The American Institute of Nutrition Ad Hoc Writing Committee on the Reformulation of the AIN-76A Rodent Diet recommends an n-6:n-3 ratio of no more than 7.⁵² However, due to the common use of vegetable oils as sole source of dietary fat, many commercial rodent diets have a higher n-6:n-3 ratio, with even higher ratios in Western-type diets and high-fat, high-cholesterol diets. In our study, the high-fat diet had a n-6:n-3 ratio of 13.9 and the control diet had a n-6:n-3 ratio of 8.4, both of which are well above the American Institute of Nutrition recommended levels.⁵² High consumption of long-chain fatty acids of the omega-6 family by humans is a risk factor for allergic diseases, including atopic dermatitis.^{27,28} An imbalance between n-6 and n-3 fatty acids is assumed to increase production of proinflammatory mediators and to shift toward a Th2 and Th17 response.³⁵ In addition, high levels of n-6 polyunsaturated fatty acids promote mast cell degranulation.^{25,27,28} Because most UD treatments do not involve a change in diet, this feature may underlie the partial response reported in the literature for different treatments, given, that the stimuli for the mast cell degranulation persist.^{1,2,18,27–29,35,40,44,46,63} In addition, as B6 mice accumulate subcutaneous fat, white adipocytes become larger; this change may be accompanied by insufficient vascularization and oxygen supply, leading to oxidative stress and hypoxia-induced inflammation in the adipose tissue.⁴⁷ Furthermore, adipose tissue produces IL6 and TNF α , which promote Th17 cell differentiation.^{13,26,45} Mast cells and Th17 cells present in adipose tissue increase in number during the course of obesity.^{19,43} Together with fatty acids and products derived from adipocyte cell death, inflammatory cytokines and chemokines promote the accumulation and activation of inflammatory cells in adipose tissue, leading to inflammation of adipose tissue.^{13,26,45} Therefore, inflammation of adipose tissue may contribute to UD in obese B6 mice.

Our study showed that a high-fat diet is associated with mast cell degranulation in female B6 mice. In addition, total skin

mast cell numbers and degranulation rates increase with age in female B6 mice regardless of diet. A limitation of our study was the use of only female B6 mice. We used this strain because it is one of the most commonly used across research institutions and because studies report that females are more commonly affected by UD than are males.^{9,61} In addition, females are reported to develop UD at an earlier age than males; this propensity was useful because we were not able to perform a long-term study.⁶¹ A similar study using both sexes for a longer duration could help to more clearly define UD etiopathogenesis in both sexes.

In summary, our findings suggest mast cell degranulation is the initiating event leading to UD in B6 female mice, and treatments directed at preventing mast cell degranulation may result in better outcomes when applied early in UD cases. In addition, a direct correlation links dietary fat and skin mast cell degranulation, with total skin mast cell numbers and degranulation rates increasing with age in female C57BL/6J mice. As noted previously in studies using caloric restriction, a lower fat content in rodent diets may help to prevent UD in B6 mice.

Acknowledgments

This study was supported by the Intramural Research Program of the NIH, National Institute of Allergy and Infectious Diseases, Laboratory of Immunogenetics, Comparative Medicine Branch, the Biostatistics Research Branch, and the Pathology Service, Office of Research Services.

References

1. Adams SC, Garner JP, Felt SA, Geronimo JT, Chu DK. 2016. A 'pedi' cures all: Toenail trimming and the treatment of ulcerative dermatitis in mice. *PLoS One* 11:e0144871. <https://doi.org/10.1371/journal.pone.0144871>.
2. Alvarado CG, Franklin CL, Dixon LW. 2016. Retrospective evaluation of nail trimming as a conservative treatment for ulcerative dermatitis in laboratory mice. *J Am Assoc Lab Anim Sci* 55:462–466.
3. *American Veterinary Medical Association*. 2013. Guidelines for the euthanasia of animals, 2013 edition.
4. Andoh T, Yageta Y, Takeshima H, Kuraishi Y. 2004. Intradermal nociceptin elicits itch-associated responses through leukotriene B(4) in mice. *J Invest Dermatol* 123:196–201. <https://doi.org/10.1111/j.0022-202X.2004.22704.x>.
5. Andrews AG, Dysko RC, Spilman SC, Kunkel RG, Brammer DW, Johnson KJ. 1994. Immune complex vasculitis with secondary ulcerative dermatitis in aged C57BL/6N mice. *Vet Pathol* 31:293–300. <https://doi.org/10.1177/030098589403100301>.
6. Animal Welfare Act as Amended. 2013. 7 USC § 2131–2159.
7. Animal Welfare Regulations. 2013. 9 CFR § 3.75–3.92.
8. Ashida Y, Denda M, Hirao T. 2001. Histamine H1 and H2 receptor antagonists accelerate skin barrier repair and prevent epidermal hyperplasia induced by barrier disruption in a dry environment. *J Invest Dermatol* 116:261–265. <https://doi.org/10.1046/j.1523-1747.2001.01238.x>.
9. Blackwell BN, Bucci TJ, Hart RW, Turturro A. 1995. Longevity, body weight, and neoplasia in ad libitum-fed and diet-restricted C57BL/6 mice fed NIH31 open-formula diet. *Toxicol Pathol* 23:570–582. <https://doi.org/10.1177/019262339502300503>.
10. Bourre JM, Francois M, Youyou A, Dumont O, Piciotti M, Pascal G, Durand G. 1989. The effects of dietary alpha-linolenic acid on the composition of nerve membranes, enzymatic activity, amplitude of electrophysiological parameters, resistance to poisons and performance of learning tasks in rats. *J Nutr* 119:1880–1892. <https://doi.org/10.1093/jn/119.12.1880>.
11. Bourre JM, Piciotti M, Dumont O, Pascal G, Durand G. 1990. Dietary linoleic acid and polyunsaturated fatty acids in rat brain and other organs. Minimal requirements of linoleic acid. *Lipids* 25:465–472. <https://doi.org/10.1007/BF02538090>.
12. Brown MA. 2018. Studies of mast cells: Adventures in serendipity. *Front Immunol* 9:520. <https://doi.org/10.3389/fimmu.2018.00520>.

13. **Chmelar J, Chung KJ, Chavakis T.** 2013. The role of innate immune cells in obese adipose tissue inflammation and development of insulin resistance. *Thromb Haemost* **109**:399–406. <https://doi.org/10.1160/TH12-09-0703>.
14. **Csiza CK, McMartin DN.** 1976. Apparent acaridal dermatitis in a C57BL/6 Nya mouse colony. *Lab Anim Sci* **26**:781–787.
15. **De Biase D, Esposito F, De Martino M, Pirozzi C, Luciano A, Palma G, Raso GM, Iovane V, Marzocco S, Fusco A, Paciello O.** 2019. Characterization of inflammatory infiltrate of ulcerative dermatitis in C57BL/6Ncrl-Tg(HMGA1P6)1Pg mice. *Lab Anim* **53**:447–458. <https://doi.org/10.1177/0023677218815718>.
16. **Duarte-Vogel SM, Lawson GW.** 2011. Association between hair-induced oronasal inflammation and ulcerative dermatitis in C57BL/6 mice. *Comp Med* **61**:13–19.
17. **Dunn TB.** 1954. The importance of differences in morphology in inbred strains. *J Natl Cancer Inst* **15**:573–591.
18. **Ezell PC, Papa L, Lawson GW.** 2012. Palatability and treatment efficacy of various ibuprofen formulations in C57BL/6 mice with ulcerative dermatitis. *J Am Assoc Lab Anim Sci* **51**:609–615.
19. **Fabbrini E, Cella M, McCartney SA, Fuchs A, Abumrad NA, Pietka TA, Chen Z, Finck BN, Han DH, Magkos F, Conte C, Bradley D, Fraterrigo G, Eagon JC, Patterson BW, Colonna M, Klein S.** 2013. Association between specific adipose tissue CD4+ T-cell populations and insulin resistance in obese individuals. *Gastroenterology* **145**:366–374. <https://doi.org/10.1053/j.gastro.2013.04.010>.
20. **Furue K, Ito T, Tanaka Y, Yumine A, Hashimoto-Hachiya A, Take-mura M, Murata M, Yamamura K, Tsuji G, Furue M.** 2019. Cyto/chemokine profile of in vitro scratched keratinocyte model: Implications of significant upregulation of CCL20, CXCL8 and IL36G in Koebner phenomenon. *J Dermatol Sci* **94**:244–251. <https://doi.org/10.1016/j.jdermsci.2019.04.002>.
21. **Garcovich S, Maurelli M, Gisondi P, Peris K, Yosipovitch G, Girolomoni G.** 2021. Pruritus as a distinctive feature of type 2 inflammation. *Vaccines (Basel)* **9**:303. <https://doi.org/10.3390/vaccines9030303>.
22. **Glatzer F, Gschwandtner M, Ehling S, Rossbach K, Janik K, Klos A, Bäumer W, Kietzmann M, Werfel T, Gutzmer R.** 2013. Histamine induces proliferation in keratinocytes from patients with atopic dermatitis through the histamine 4 receptor. *J Allergy Clin Immunol* **132**:1358–1367. <https://doi.org/10.1016/j.jaci.2013.06.023>.
23. **Gri G, Frossi B, D'Inca F, Danelli L, Betto E, Mion F, Sibillano R, Pucillo C.** 2012. Mast cell: An emerging partner in immune interaction. *Front Immunol* **3**:120. <https://doi.org/10.3389/fimmu.2012.00120>.
24. **Gueck T, Aschenbach JR, Fuhrmann H.** 2002. Influence of vitamin E on mast cell mediator release. *Vet Dermatol* **13**:301–305. <https://doi.org/10.1046/j.1365-3164.2002.00307.x>.
25. **Gueck T, Seidel A, Fuhrmann H.** 2003. Effects of essential fatty acids on mediators of mast cells in culture. *Prostaglandins Leukot Essent Fatty Acids* **68**:317–322. [https://doi.org/10.1016/S0952-3278\(03\)00022-X](https://doi.org/10.1016/S0952-3278(03)00022-X).
26. **Guo Z, Yang Y, Liao Y, Shi Y, Zhang LJ.** 2022. Emerging roles of adipose tissue in the pathogenesis of psoriasis and atopic dermatitis in obesity. *JID Innov* **2**:100064. <https://doi.org/10.1016/j.xjidi.2021.100064>.
27. **Hagemann PM, Nsiah-Dosu S, Hundt JE, Hartmann K, Orinska Z.** 2019. Modulation of mast cell reactivity by lipids: The neglected side of allergic diseases. *Front Immunol* **10**:1174. <https://doi.org/10.3389/fimmu.2019.01174>.
28. **Hagenlocher Y, Lorentz A.** 2015. Immunomodulation of mast cells by nutrients. *Mol Immunol* **63**:25–31. <https://doi.org/10.1016/j.molimm.2013.12.005>.
29. **Hampton AL, Aslam MN, Naik MK, Bergin IL, Allen RM, Craig RA, Kunkel SL, Veerapaneni I, Paruchuri T, Patterson KA, Rothman ED, Hish GA, Varani J, Rush HG.** 2015. Ulcerative dermatitis in C57BL/6Ncrl mice on a low-fat or high-fat diet with or without a mineralized red-algae supplement. *J Am Assoc Lab Anim Sci* **54**:487–496.
30. **Hampton AL, Hish GA, Aslam MN, Rothman ED, Bergin IL, Patterson KA, Naik M, Paruchuri T, Varani J, Rush HG.** 2012. Progression of ulcerative dermatitis lesions in C57BL/6Crl mice and the development of a scoring system for dermatitis lesions. *J Am Assoc Lab Anim Sci* **51**:586–593.
31. **Harvima IT, Nilsson G.** 2011. Mast cells as regulators of skin inflammation and immunity. *Acta Derm Venereol* **91**:644–650. <https://doi.org/10.2340/00015555-1197>.
32. **Humeau M, Boniface K, Bodet C.** 2022. Cytokine-mediated cross-talk between keratinocytes and T cells in atopic dermatitis. *Front Immunol* **13**:801579. <https://doi.org/10.3389/fimmu.2022.801579>.
33. *Institute for Laboratory Animal Research.* 2011. Guide for the care and use of laboratory animals, 8th edition. Washington (DC): National Academies Press.
34. **Jacobi A, Antoni C, Manger B, Schuler G, Hertl M.** 2005. Infliximab in the treatment of moderate to severe atopic dermatitis. *J Am Acad Dermatol* **52**:522–526. <https://doi.org/10.1016/j.jaad.2004.11.022>.
35. **Jena PK, Sheng L, Mcneil K, Chau TQ, Yu S, Kiuru M, Fung MA, Hwang ST, Wan YY.** 2019. Long-term Western diet intake leads to dysregulated bile acid signaling and dermatitis with Th2 and Th17 pathway features in mice. *J Dermatol Sci* **95**:13–20. <https://doi.org/10.1016/j.jdermsci.2019.05.007>.
36. **Kesterson K, Nahmias Z, Brestoff JR, Bodet ND, Kau A, Kim BS.** 2018. Generalized pruritus relieved by NSAIDs in the setting of mast cell activation syndrome. *J Allergy Clin Immunol Pract* **6**:2130–2131. <https://doi.org/10.1016/j.jaip.2018.03.002>.
37. **Kitagaki M, Hirota M.** 2007. Auricular chondritis caused by metal ear tagging in C57BL/6 mice. *Vet Pathol* **44**:458–466. <https://doi.org/10.1354/vp.44-4-458>.
38. **Krugner-Higby L, Brown R, Rasette M, Behr M, Okwumabua O, Cook M, Bell C, Flowers MT, Ntambi J, Gendron A.** 2012. Ulcerative dermatitis in C57BL/6 mice lacking stearoyl CoA desaturase 1. *Comp Med* **62**:257–263.
39. **Krynicka K, Trzeciak M.** 2022. The role of sodium hypochlorite in atopic dermatitis therapy: A narrative review. *Int J Dermatol* **61**:1080–1086. <https://doi.org/10.1111/ijd.16099>.
40. **Lawson GW, Sato A, Fairbanks LA, Lawson PT.** 2005. Vitamin E as a treatment for ulcerative dermatitis in C57BL/6 mice and strains with a C57BL/6 background. *Contemp Top Lab Anim Sci* **44**:18–21.
41. **Lee KS, Chun SY, Lee MG, Kim S, Jang TJ, Nam KS.** 2018. The prevention of TNF- α /IFN- γ mixture-induced inflammation in human keratinocyte and atopic dermatitis-like skin lesions in Nc/Nga mice by mineral-balanced deep sea water. *Biomed Pharmacother* **97**:1331–1340. <https://doi.org/10.1016/j.biopha.2017.11.056>.
42. **Lee JH, Fukumoto M, Nishida H, Ikeda I, Sugano M.** 1989. The interrelated effects of n-6/n-3 and polyunsaturated/saturated ratios of dietary fats on the regulation of lipid metabolism in rats. *J Nutr* **119**:1893–1899. <https://doi.org/10.1093/jn/119.12.1893>.
43. **Liu J, Divoux A, Sun J, Zhang J, Clément K, Glickman JN, Sukhova GK, Wolters PJ, Du J, Gorgun CZ, Doria A, Libby P, Blumberg RS, Kahn BB, Hotamisligil GS, Shi GP.** 2009. Genetic deficiency and pharmacological stabilization of mast cells reduce diet-induced obesity and diabetes in mice. *Nat Med* **15**:940–945. <https://doi.org/10.1038/nm.1994>.
44. **Mader JR, Mason MA, Bale LK, Gades NM, Conover CA.** 2010. The association of early dietary supplementation with vitamin E with the incidence of ulcerative dermatitis in mice on a C57BL/6 background: Diet and ulcerative dermatitis in mice. *Scand J Lab Anim Sci* **37**:253–259.
45. **Majewska-Szczepanik M, Kowalczyk P, Marcińska K, Strzępa A, Lis GJ, Wong FS, Szczepanik M, Wen L.** 2022. Obesity aggravates contact hypersensitivity reaction in mice. *Contact Dermatitis* **87**:28–39. <https://doi.org/10.1111/cod.14088>.
46. **Michaud CR, Qin J, Elkins WR, Gozalo AS.** 2016. Comparison of 3 topical treatments against ulcerative dermatitis in mice with a C57BL/6 background. *Comp Med* **66**:100–104.
47. **Monji A, Zhang Y, Kumar GVN, Guillermier C, Kim S, Olenchock B, Steinhauser ML.** 2022. A cycle of inflammatory adipocyte death and regeneration in murine adipose tissue. *Diabetes* **71**:412–423. <https://doi.org/10.2337/db20-1306>.
48. **Murakami S, Futamura K, Matsumoto K, Adachi Y, Matsuda A.** 2022. An epidermal keratinocyte homogenate induced type 2 and proinflammatory cytokine expression in cultured der-

- mal cells. *J Dermatol Sci* **106**:93–100. <https://doi.org/10.1016/j.jdermsci.2022.04.002>.
49. **Murphy ED**. 1977. Effects of mutant steel alleles on leukemogenesis and life-span in the mouse. *J Natl Cancer Inst* **58**:107–110. <https://doi.org/10.1093/jnci/58.1.107>.
 50. **Neuhaus B, Niessen CM, Mesaros A, Withers DJ, Krieg T, Partridge L**. 2012. Experimental analysis of risk factors for ulcerative dermatitis in mice. *Exp Dermatol* **21**:712–713. <https://doi.org/10.1111/j.1600-0625.2012.01558.x>.
 51. **Perkins SN, Hursting SD, Phang JM, Haines DC**. 1998. Calorie restriction reduces ulcerative dermatitis and infection-related mortality in p53-deficient and wildtype mice. *J Invest Dermatol* **111**:292–296. <https://doi.org/10.1046/j.1523-1747.1998.00270.x>.
 52. **Reeves PG, Nielsen FH, Fahey GC**. 1993. AIN-93 purified diets for laboratory rodents: Final report of the American Institute of Nutrition Ad Hoc Writing Committee on the Reformulation of the AIN-76A Rodent Diet. *J Nutr* **123**:1939–1951. <https://doi.org/10.1093/jn/123.11.1939>.
 53. **Sargent JL, Koewler NJ, Diggs HE**. 2015. Systematic literature review of risk factors and treatments for ulcerative dermatitis in C57BL/6 mice. *Comp Med* **65**:465–472.
 54. **Sargent JL, Löhr CV, Diggs HE**. 2016. Scratching responses to epidermal injury in C57BL/6, DBA/2, BALB/c, and CD1 mice. *Comp Med* **66**:208–215.
 55. **Smith SE, Maus RL, Davis TR, Sundberg JP, Gil D, Schrum AG**. 2016. Maternal IL-6 can cause T-cell-mediated juvenile alopecia by non-scarring follicular dystrophy in mice. *Exp Dermatol* **25**:223–228. <https://doi.org/10.1111/exd.12914>.
 56. **Stowe HD, Wagner JL, Pick JR**. 1971. A debilitating fatal murine dermatitis. *Lab Anim Sci* **21**:892–897.
 57. **Sundberg JP, Taylor D, Lorch G, Miller J, Silva KA, Sundberg BA, Roopenian D, Sperling L, Ong D, King LE, Everts H**. 2011. Primary follicular dystrophy with scarring dermatitis in C57BL/6 mouse substrains resembles central centrifugal cicatricial alopecia in humans. *Vet Pathol* **48**:513–524. <https://doi.org/10.1177/0300985810379431>.
 58. **Suto H, Nambu A, Morita H, Yamaguchi S, Numata T, Yoshizaki T, Shimura E, Arae K, Asada Y, Motomura K, Kaneko M, Abe T, Matsuda A, Iwakura Y, Okumura K, Saito H, Matsumoto K, Sudo K, Nakae S**. 2018. IL-25 enhances TH17 cell-mediated contact dermatitis by promoting IL-1 β production by dermal dendritic cells. *J Allergy Clin Immunol* **142**:1500–1509. <https://doi.org/10.1016/j.jaci.2017.12.1007>.
 59. **Toyoshima S, Okayama Y**. 2022. Neuro-allergology: Mast cell-nerve cross-talk. *Allergol Int* **71**:288–293. <https://doi.org/10.1016/j.alit.2022.04.002>.
 60. **Tsukamoto A, Ohgoda M, Haruki N, Hori M, Inomata T**. 2018. The anti-inflammatory action of maropitant in a mouse model of acute pancreatitis. *J Vet Med Sci* **80**:492–498. <https://doi.org/10.1292/jvms.17-0483>.
 61. **Turturro A, Duffy P, Hass B, Kodell R, Hart R**. 2002. Survival characteristics and age-adjusted disease incidences in C57BL/6 mice fed a commonly used cereal-based diet modulated by dietary restriction. *J Gerontol A Biol Sci Med Sci* **57**:B379–B389. <https://doi.org/10.1093/gerona/57.11.B379>.
 62. **Williams LK, Csaki LS, Cantor RM, Reue K, Lawson GW**. 2012. Ulcerative dermatitis in C57BL/6 mice exhibits an oxidative stress response consistent with normal wound healing. *Comp Med* **62**:166–171.
 63. **Williams-Fritze MJ, Carlson Scholz JA, Zeiss C, Deng Y, Wilson SR, Franklin R, Smith PC**. 2011. Maropitant citrate for treatment of ulcerative dermatitis in mice with a C57BL/6 background. *J Am Assoc Lab Anim Sci* **50**:221–226.
 64. **Yamamoto M, Haruna T, Ueda C, Asano Y, Takahashi H, Iduhara M, Takaki S, Yasui K, Matsuo Y, Arimura A**. 2009. Contribution of itch-associated scratch behavior to the development of skin lesions in *Dermatophagoides farinae*-induced dermatitis model in NC/Nga mice. *Arch Dermatol Res* **301**:739–746. <https://doi.org/10.1007/s00403-008-0912-8>.
 65. **Zemel MB, Sun X**. 2008. Dietary calcium and dairy products modulate oxidative and inflammatory stress in mice and humans. *J Nutr* **138**:1047–1052. <https://doi.org/10.1093/jn/138.6.1047>.